Requirements for artificial muscles to design robotic fingers

J. L. Ramírez, A. Rubiano, N. Jouandeau, L. Gallimard and O. Polit

Abstract This work is part of the ProMain project that concerns the modeling and the design of a soft robotic hand prosthesis, actuated by artificial muscles and controlled with surface Electromyography (EMG) signals. In a first stage, we designed a robotic finger based on the equivalent mechanical model of the human finger. The model takes into account three phalangeal joints, flexion and extension movements are studied. The robotic finger has three Degrees of Freedom (DoF). The finger is designed to be under-actuated and driven by tendons, *i.e.* only one servo motor actuates the whole finger, and the motor is coupled to the finger mechanism through two flexible wires. As the aim is to design a robotic hand prosthesis that uses artificial muscles, we propose and carry out two experiments to characterize the specifications of the actuator. The first experiment measures the pinch force of the human finger, and the second measures the achieved force using our robotic finger and five different servo motors. It allows us to enhance experimental results with the mathematical model of the finger, to identify the requirements of the artificial muscle.

1 Introduction

In the domain of robotic prostheses, the main challenge is the design of well sized mechatronic limbs and smart controllers that should help people to achieve desired movements. Up to now, several robotic hands have been designed to accomplish dexterous manipulation tasks, imitating the behavior of the human hand. One example is the KH Hand [1], which is anthropomorphic, uses DC motors and has

J. L. Ramírez, A. Rubiano, L. Gallimard and O. Polit
LEME, Université Paris Ouest Nanterre le Défense, 50 rue de Sèvres 92410 Ville d'Avray - France,
e-mail: jl.ramirez_arias@u-paris10.fr

N. Jouandeau
LIASD, Université Paris 8, 2, Rue de la Liberté, 93526 Saint-Denis - France,
e-mail: n@ai.univ-paris8.fr

five fingers and 15 Degrees of Freedom (DoF). Likewise, the Shadow Hand [2] has five fingers and 20 DoF, and uses pneumatic actuators. Furthermore, the HIRO III hand [3] has 15 DoF and is actuated by DC motors, and has an interesting application because it was designed to be a haptic device with force feedback in the fingertips.

However, despite their potential, the hands present in the state of the art have drawbacks that hinder them to be used as a hand prostheses. The main disadvantage is the rigid behavior. The human hand is versatile and due to its adaptability and flexibility it is able to achieve different tasks in an accurate way. Consequently, to design a robotic hand prosthesis, it is necessary to add adaptability and flexibility as a main design requirement.

The utilization of smart and soft materials has led to the development of new adaptive devices (known as soft robots [4]) for physical rehabilitation and improvement of human skills. Particularly in the field of soft robotic hands, some works have been conducted: the UB Hand [5] and the Pisa/IIT hand [6], which are good examples of the development achieved. Even the DLR Hand II [7] can be considered to has a soft behavior due to its driving mechanism that is based on tendons.

Concerning the smart materials for artificial muscles, significant studies are currently being pulled off to develop new actuation strategies, but these technologies are still far from implementation in anthropomorphic robotic hands [8]. The first step in the development of artificial muscles for a robotic hand prosthesis is the determination of the actuator requirements. Consequently, ProMain project intends the development of a soft robotic hand prosthesis, with artificial muscles and a control system based on surface EMG signals.

The artificial muscle's requirements are closely related to the robot's features as the used mechanism, the desired level of softness, and the task to be performed. Therefore, it is necessary to develop a mathematical model to describe the robot and the task, allowing the analysis in a more general way. The mathematical models for robotic hands are based on the kinematic and dynamic analysis of its articulated chains. Usually, the Denavit-Hartemberg (DH) parameters [9] are used to model any kind of articulated chains. The main drawback of the DH parameters utilization is the limitation of active rotations because they are only possible around $z-axes$ of each reference, and a new frame must be added if an extra rotation is needed. Furthermore, the use of homogeneous matrices can cause singularities due to the presence of non-considered rotations introduced with soft materials.

Therefore, in this paper, we adopt the kinematic model DHKK-SRQ [10], that allows to know the complete kinematic of the finger, considering the soft behavior of the robot. The model uses the so-called DHKK convention [11] (which corresponds to the DH parameters, modified by Khalil and Kleinfinger) and express the soft rotations using quaternions. Concerning the task to be performed, the interaction with the object is very important, and it is usually modeled using the postural [5] and the adaptive synergies [6]. The DHKK-SRQ also takes into account the shape and inertial forces of manipulated objects. The proposed dynamic model uses the principle of virtual displacements and virtual works [12].

Artificial muscle's requirements are linked with the robot mechanism, so we use the finger of the ProMain-I [10] hand as the prototype. This finger is the result of a morphological optimization process [12] and consists of three phalangeal joints with flexion - extension, (*i.e.* 3 DoF). The finger is designed to be under-actuated and driven by tendons, so, only one servo motor actuates the whole finger, and the motor is coupled to the mechanism through flexible wires.

Two experiments are presented to identify the actuation characteristics, the first measures the human force and the second evaluates if classical servo motors fulfill the human hand requirements. The second experiment consists of two stages as follows:

1. Test the finger with five different servo motors, measuring the fingertip force and calculating the motor torque using the kinematic and dynamic model.
2. Measure the pinch force, using a test platform where two fingers are placed facing each other (in pinch position), to validate that the grasping force corresponds to the double of the fingertip force.

Experimental data are analyzed using the kinematic and dynamic models to define the characteristics of the artificial muscle. The obtained results indicate that new actuation technologies can fulfill the force, speed and displacement requirements of a robotic hand prosthesis. This progress is encouraging and permits to follow new directions in the research of smart materials for artificial muscles in robotic hands.

Furthermore, the layout of this paper is as follows. First in section 2, we introduce our finger prototype and its modeling. Then, section 3 shows the experimental set-up and the measures. Subsequently, section 4 exposes the data analysis and the definition of the artificial muscle requirements.

2 Under actuated Robotic Finger ProMain-I

Our prototype is a bio-inspired tendon-driven finger [12] composed of three joints: the metacarpophalangeal (MP), the proximal interphalangeal (PIP) and the distal interphalangeal (DIP). All the joints have one DoF to perform flexion and extension. The finger is controlled by only one servo motor, and the drive mechanism uses two tendons for transmitting motion, one for the flexion and one for the extension, as shown in Figure 1. Considering that the tendons are fastened to the motor pulley and the fingertip, the clockwise rotation of the actuator produces the flexion, and the counterclockwise rotation produces the extension.

Due to the under actuation, the rotation angle of the PIP and DIP joints are linked with the rotation angle of the MP joint. The relation between the angles is approximated with $\theta_2 = 0.23\theta_1$ and $\theta_3 = 0.72\theta_1$, where θ_1 is the MP joint angle, θ_2 is the PIP joint angle and θ_3 is the DIP joint angle. Furthermore, the parameters l_1, l_2 and l_3 are the lengths of the proximal, medial and distal phalanges, as shown in Figure 1. For the kinematic analysis, the hybrid DHKK-SRQ model [10] is used, and the dy-

namic model uses the virtual displacements and the virtual works approach [12]. The kinematic and the dynamic models are presented in the following subsections.

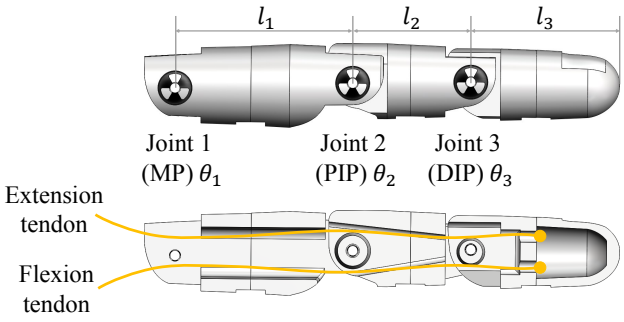

Figure 1: Finger mechanism.

2.1 kinematic model of the ProMain-I finger

The DHKK convention, allows the representation of open-loop and close-loop kinematic chains, and presents a convenient definition of the axes z_i, which corresponds to the rotation axis of the i^{th} joint. The angle of rotation around z_i is denoted by θ_i, and is applied using the transformation matrix that is described in Eq. (1). The matrix ${}^{i-1}T_i$ results of the application of: 1) a rotation α_i around x_{i-1}, 2) a translation a_i along of x_{i-1}, 3) a rotation θ_i around z_i and 4) a translation d_i along of z_i [11]. The parameters α_i, a_i, θ_i and d_i, are known as the DHKK parameters, a graphical representation of the parameters is shown in Figure 2.

$$ {}^{i-1}T_i = \begin{bmatrix} \cos\theta_i & \sin\theta_i & 0 & a_i \\ \sin\theta_i\cos\alpha_i & \cos\theta_i\cos\alpha_i & \sin\alpha_i & \sin\alpha_i d_i \\ \sin\theta_i\sin\alpha_i & \cos\theta_i\sin\alpha_i & \cos\alpha_i & \cos\alpha_i d_i \\ 0 & 0 & 0 & 1 \end{bmatrix} \tag{1} $$

Consequently, the kinematic of a robot composed of n joints is the matrix ${}^0T_n$, which is a composition of the orientation of the end effector ${}^0R_n$, and the position vector $[{}^0P_n^x, {}^0P_n^y, {}^0P_n^z]$, as shown in the following expression:

$$ {}^0T_n = \prod_{i=1}^{n} {}^{i-1}T_i = \left[\begin{array}{ccc|c} & & & {}^0P_n^x \\ & {}^0R_n & & {}^0P_n^y \\ & & & {}^0P_n^z \\ \hline 0 & 0 & 0 & 1 \end{array}\right] \tag{2} $$

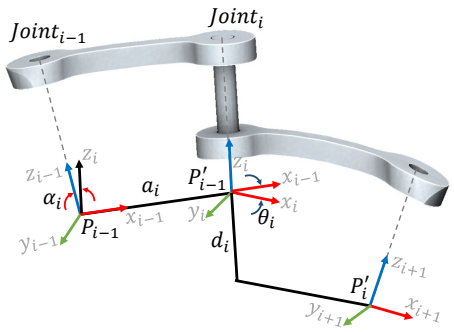

Figure 2: Graphical representation of DHKK parameters [10].

We consider a quaternion as a vector represented in the hypersphere S^3[13], which is centered at the origin of the frame. We represent a rotation of a vector $\mathbf{r}$, with value γ, around the vector $\mathbf{n}$ as $\mathbb{N}\mathbb{R}\overline{\mathbb{N}}$, where $\mathbb{N} = [\![\cos(\gamma/2), \mathbf{n}\sin(\gamma/2)]\!]$ is the quaternion that corresponds to the vector $\mathbf{n}$, $\mathbb{R} = [\![0, \mathbf{r}]\!]$ is the quaternion that correspond to the vector $\mathbf{r}$, and $\overline{\mathbb{N}}$ is the conjugate of the quaternion $\mathbb{N}$.

Likewise, in the 3D space, a group of rotations with angles α, β, θ applied to the vector $\mathbf{r}$ around the axes x, y, z, as shown in Figure 3, is expressed as:

$$\mathbb{X}\mathbb{Y}\mathbb{Z}\mathbb{R}\overline{\mathbb{X}\mathbb{Y}\mathbb{Z}} \tag{3}$$

where $\mathbb{X} = [\![\cos(\alpha/2), \mathbf{x}\sin(\alpha/2)]\!]$
$\mathbb{Y} = [\![\cos(\beta/2), \mathbf{y}\sin(\beta/2)]\!]$
$\mathbb{Z} = [\![\cos(\theta/2), \mathbf{z}\sin(\theta/2)]\!]$

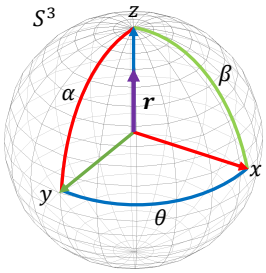

Figure 3: Combination of rotations α, β and θ of $\pi/2$ *rad* around x, y and z. [10].

The hybrid model DHKK-SRQ unifies the DHKK parameters with multiple sets of quaternions, using an optimal analysis of the available sensor feedback. Thus, each i^{th} joint (for $i = 1, \ldots, n$ where n is the number of joints) is considered as an element that has a hybrid (*i.e.* rigid and soft) behavior. Consequently, the i^{th}

joint is modeled, in a first step as a rigid element, with only the rotation θ_i around z_i. Subsequently, the rotations α_i and β_i around axis x_i and y_i are added using the hypersphere S_i^3 centered in the joint frame. As a result, the model can apply rotations in all axes avoiding to add any extra reference frame.

Initially, the rotations are performed using the homogeneous matrices that are given by Eq. (1), and the kinematic of the rigid joints results from Eq. (2). Afterwards, we formulate the extra rotations (those that appear from the low stiffness joints) α_i and β_i using SRQ. Additionally, if SRQ is active, then the rotation θ_i is formulated using a quaternion; so that, the set of quaternions for each i^{th} joint is like the proposed in Eq. (3). The equivalent kinematic model of the finger is shown in Figure 4.

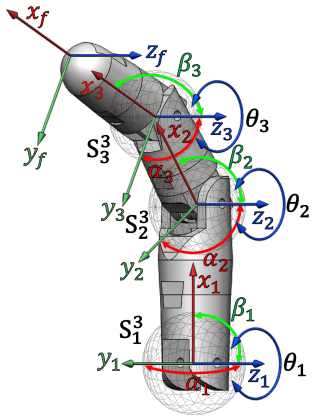

Figure 4: kinematic model of the robotic finger.

The frame (x_1, y_1, z_1) and the hypersphere S_1^3 are associated to the joint 1 (MP). The frame (x_2, y_2, z_2) and the hypersphere S_2^3 are associated to the joint 2 (PIP). And the frame (x_3, y_3, z_3) and the hypersphere S_3^3 are associated to the joint 3 (DIP). The frame (x_f, y_f, z_f) corresponds to the fingertip position. Table 1 shows the DHKK parameters of the ProMain-I finger.

i	α	a	d	θ
1	0	0	0	θ_1
2	0	l_1	0	θ_2
3	0	l_2	0	θ_3
f	0	l_3	0	0

Table 1: DHKK parameters of the ProMain-I Finger.

2.2 Dynamic model of the ProMain-I finger

The equivalent dynamic model of the finger is shown in Figure 5. w_1, w_2 and w_3 are respectively the weights of the proximal, medial and distal phalanges, and are placed at the coordinates (x'_1, y'_1), (x'_2, y'_2) and (x'_3, y'_3). f_R is the applied force that is equivalent to the reaction force.

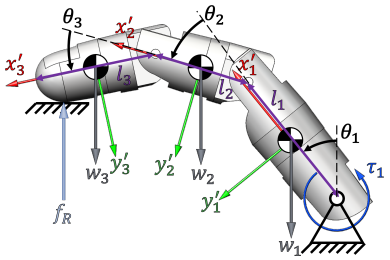

Figure 5: Dynamic model of the robotic finger.

The proposed dynamic model uses the principle of the virtual displacements and virtual works [12]. The virtual work δW is calculated for the external forces (*e.g.* weight, applied force and input torque) in Eq. (4) and the inertial forces (*e.g.* centrifugal forces) in Eq. (5).

$$\delta W_e = Q_e^T \delta r_e \tag{4}$$

where Q_e^T is the external forces vector and δr_e is the virtual displacement vector of the forces application points.

$$\delta W_\iota = M\ddot{q}^T \delta r_\iota \tag{5}$$

where M is the diagonal mass matrix composed with the masses m_i and inertias J_i. The index i is used to denote the i^{th} joint, and the index ι (*i.e.* without dot) is used to notice the independent coordinates. $\ddot{q}^T$ is the second derivate with respect to the time of the q vector shown in Eq. (6), and represents the acceleration vector. And δr_ι is the virtual displacement vector of the inertial frameworks.

$$q = [x'_1, y'_1, \theta_1, x'_2, y'_2, \theta_2, x'_2, y'_2, \theta_1] \tag{6}$$

The dynamic equilibrium is given by $\delta q^T [M\ddot{q} - Q_e] = 0$ when substituting Eq. (4) and Eq. (5) in $\delta W_e = \delta W_\iota$. In order to solve the equilibrium equation, considering the movements restrictions, it is necessary to separate dependent and independent coordinates. The separation is performed using the transformation proposed in Eq. (7), as result we have the equilibrium defined by Eq. (8), which is separable.

$$\delta q = B\delta q_{i\iota}, B = \begin{bmatrix} -C_{qd}^{-1} C_{q\iota} \\ I \end{bmatrix} \tag{7}$$

where C_{qd} is the jacobian of dependent coordinates, C_{qt} is the Jacobian of independent coordinates and I is the identity matrix.

$$\delta q_{it}^T B^T [M\ddot{q} - Q_e] = 0 \tag{8}$$

Solving Eq. (8), we obtain the dynamic function which gives the input torque τ_1 as function of the force f_R and the kinematic $q, \dot{q}, \ddot{q}$. The resulting expression is shown in Eq. (9), where we use the abbreviations $C_i := \cos(\theta_i)$ and $S_i := \sin(\theta_i)$.

$$\tau_1(f_R, q, \dot{q}, \ddot{q}) = \frac{H_1 - 4l_1H_{10} + H_{11}(l_2S_2 - 4)}{8l_2S_2 - 32} \tag{9}$$

where $H_1 = 2l_1^2\ddot{\theta}_1(l_2(m_2+m_1)S_2 - 4m_1 - 6m_2)S_1^2$
$H_2 = -m_2l_2^2S_2^2\ddot{\theta}_2/2$
$H_3 = ((\ddot{x}_1 + 3\ddot{\theta}_2 + 2g)m_2 + (2\ddot{\theta}_2 + g)m_3 + m_1g - 2f_R)l_2S_2$
$H_4 = (m_2l_2C_2l_1C_1\ddot{\theta}_1 + l_2^2\ddot{\theta}_2(m_2 + 2m_3)C_2^2)/4$
$H_5 = l_2(2m_3\ddot{y}_2 + m_3l_3C_3\ddot{\theta}_3 + m_2\ddot{y}_1)C_2/2 + 2m_3l_3S_3\ddot{\theta}_3$
$H_6 = (-6g - 6\ddot{x}_1)m_2 + (-4\ddot{x}_2 - 4g)m_3 + 8f_R - 4m_1g + 2J_2\ddot{\theta}_2$
$H_7 = (m_1 + 3m_2/2)l_1^2\ddot{\theta}_1C_1^2/4$
$H_8 = \ddot{\theta}_2l_2(m_2 + 2m_3/3)C_2 + 2m_3l_3C_3\ddot{\theta}_3/3$
$H_9 = 4m_3\ddot{y}_2/3 + 2m_2\ddot{y}_1$
$H_{10} = (H_2 + H_3 + H_4 + H_5 + H_6)S_1$
$H_{11} = 8(H_7 + 3l_1(H_8 + H_9)C_1/8 + J_1\ddot{\theta}_1)$

3 Experimental set-up

With the aim of defining the actuator characteristics, we held two experiments. The first measures the human pinch force, that is compared with the force achieved by a servo motor through a second test. In the following subsections, both experiments are described.

3.1 First experiment: Measure of the human hand pinch force

The pinch force can be considered as the force applied by two fingers of the hand, usually the index and the thumb fingers. The applied force must be adapted to the object's weight, acceleration, surface texture, contour and structure [14]. Consequently, the measure of the pinch force have to be customized to each problem [15], and that is why in this study we carried out an experiment suited to our requirements.

The force is measured in a group of five healthy subjects between 24 and 32 years old, all of them are males. The sensor is a hand dynamometer Vernier^{TM} D-BTA, suitable to measure the pinch force, whose characteristics are: 1) accuracy of

0.6N, 2) resolution of 0.2141N and 3) operational range from 0 to 600N. The data is collected using a digital oscilloscope connected to a computer. Figure 6 shows the scheme of the experiment. Each subject is asked to apply the maximal pinch force during a period of 15 seconds. To avoid fatigue each subject perform only three trials. Results presented in Table 2 correspond to the mean value of the pinch force performed by each subject, and the corresponding standard deviation of each measure.

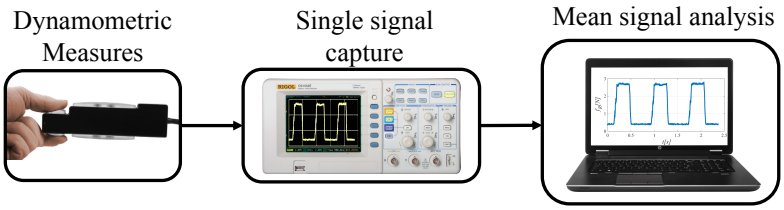

Figure 6: Experimental set-up to measure the human pinch force.

Subject	Mean pinch force [N]	Standard deviation [N]
1	6.74	0.95
2	6.45	0.08
3	4.97	0.21
4	6.71	0.71
5	4.80	0.33

Table 2: The mean value of the human pinch force.

3.2 Second experiment: Measure of the robotic finger pinch force

With the objective of establishing if a classic servo motor can fulfill the requirements of the human hand, we design two test platforms. The first one is a single-finger platform and allows to measure the kinematic and the fingertip force. The second one is a two-finger platform and consists of two fingers placed against them. It will be used to validate that the pinch force is equal to the double of the finger force. The CAD models of the test platforms are shown in Figure 7 and Figure 8.

The experiments are performed using five different servo motors, two standard and three serial, listed in Table 3. To measure the force, we used a resistive-based force sensor Flexiforce®, that measures up to 5N. The sensor is calibrated in the range of 0.6N to 4.8N and is placed on a support (platform) that is located in the trajectory of the fingertip.

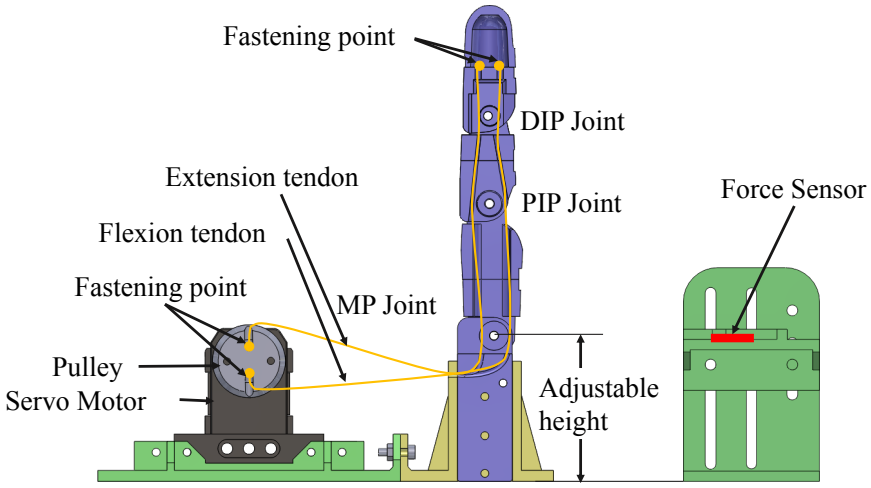

Figure 7: CAD Model of the single-finger platform.

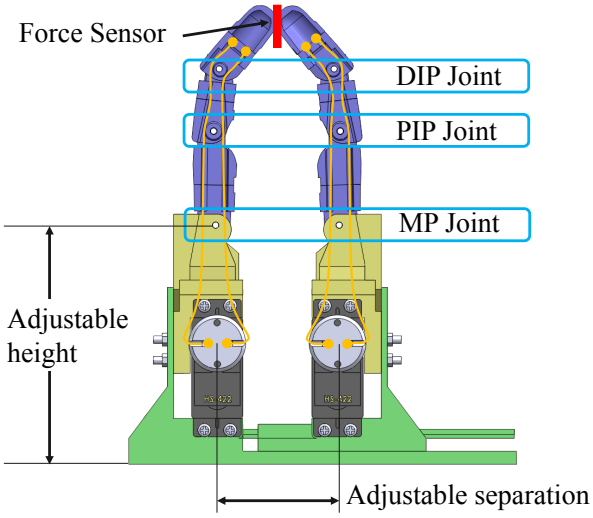

Figure 8: CAD Model of the two-finger platform.

	Reference	Maximal torque [*Nm*]
Standard servo motors	HS-422	0.324
	Traxxas-2065	0.225
Serial servo motors Dynamixel	XL-320	0.390
	AX-12a	1.50
	MX-106R	10.0

Table 3: Servo motors used in the experiments.

Furthermore, to ensure the repeatability, each servo motor is tested five times performing the same movement. Figure 9 shows the fingertip force f_R during three repetitions of flexion and extension using the HS-422 servo motor. The force applied by the MX-106R servo motor is higher than the sensor limit and also higher than mean human finger force, so its value is not taken into account. Table 4 shows the measured forces.

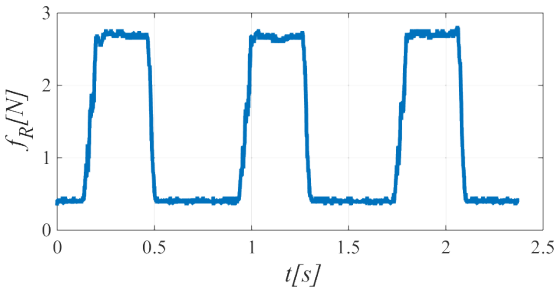

Figure 9: Results of the fingertip force using the HS-422 servo motor.

Actuator reference	**Mean fingertip force [*N*]**	**Standard deviation [*N*]**
HS-422	2.69	0.023
Traxxas-2065	1.01	0.077
AX-12a	3.21	0.024
XL-320	2.10	0.038
MX-106R	> 5	–

Table 4: Mean value of the fingertip force (one-finger platform).

The servo motor that performs the force closest to the human finger force is chosen as actuator for the two-finger platform. Consequently, we took the HS-422 servo motor for the test with the two-finger platform. Consequently, the tests with the second platform are conducted for four different distances between fingers (50, 55, 60 and 65*mm*). For each distance the test is carried out five times. Table 5 shows the measured grip force using the two-finger platform.

Distance [*mm*]	**Mean pinch Force [*N*]**	**Standard deviation [*N*]**
50	4.02	0.02
55	4.62	0.08
60	4.70	0.05
65	3.54	0.06

Table 5: Mean pinch force (two-finger platform).

Considering that the finger performs flexion and extension in 2D, the kinematic is measured using a high-performance CCD camera Prosilica GE-2040, which tracks black markers placed on the finger joints and the fingertip. Figure 10 shows the scheme of the experiment. The kinematic data is correlated with the DHKK-SRQ and the dynamic model to identify the torque and displacement requirements of artificial muscles. Kinematic results are presented and analyzed in the next section.

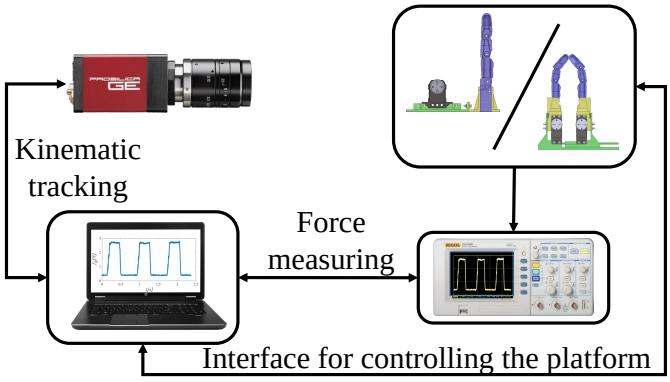

Figure 10: Experimental set-up to track the kinematic and measure applied force of the robotic finger.

4 Requirements and characterization of the artificial muscle

The main features of an actuator are the force, strain and time response. Thus, we need to define these characteristics for the artificial muscle. Considering that our goal is to design a robotic hand that will be able to perform precision grasping movement, the actuator features can be established from measures of the human hand pinch. However, it is important to take into account that the robotic finger mechanism can modify the actuator requirements. Consequently, the proposed approach, to identify the artificial muscle requirements, is defined by three kind of measures: 1) the human pinch force, 2) the human response time and 3) the kinematic and dynamic behavior of the robotic finger ProMain-I.

Pinch force requirements: Considering that our goal is to define a reference value of the human pinch force, we have collected multiple samples from each subject and computed a mean force value for each one, as shown in Table 2, section 3. Thus, the pinch force is in the interval $[4.80N, 6.74N]$, and the mean value is $5.94N$. A graphical representation of the analysis is shown in Figure 11. Furthermore, we measured the time response of the subjects, and we obtained a mean value of $0.244s$ with a standard deviation of $0.06s$.

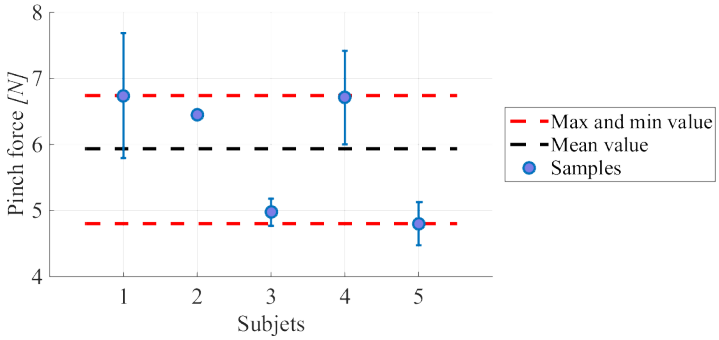

Figure 11: Human Pinch Force.

Kinematic tracking and resulting force of the ProMain-I finger: As result of the test, we get the position vectors of the joints, *i.e.* the vector $[{}^0P_1^x, {}^0P_1^y, 0]$ for the $joint_1$, $[{}^0P_2^x, {}^0P_2^y, 0]$ for the $joint_2$ and $[{}^0P_3^x, {}^0P_3^y, 0]$ for the $joint_3$. Likewise the vector $[{}^0P_f^x, {}^0P_f^y, 0]$ corresponds to the fingertip position. Considering that the movement is performed in the plan, ${}^0P_i^z$ is always zero. Figure 12 shows the results of the measured kinematic using the HS-422 servo motor.

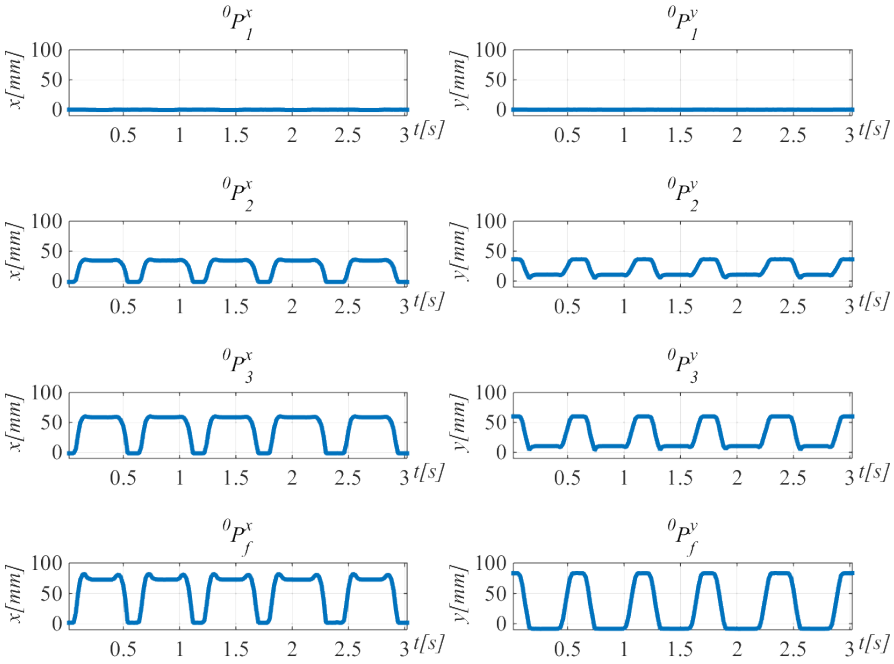

Figure 12: Results of the position tracking using the HS-422 servo motor.

The standard deviation of the measures of the MP joint (whose position is always zero) is $0.4733mm$. Likewise, the standard deviation of the measures of the joints PIP and DIP are $0.1848mm$ and $0.5598mm$ respectively. The standard deviation of the measures of the fingertip is $1.6069mm$.

Furthermore, when the test is carried out with the two-fingers platform, one finger behaves as an obstacle to the other one. Thus, the experiment shows that the relations of the angles are different from the proposed ones given in section 2. This difference in the angles behavior is not an issue as we are tracking all the movements and updating the kinematic with the DHKK-SRQ model.

Concerning the fingertip force and the pinch force, the lower difference takes place when the distance between the fingers is $60mm$. In that case, the force applied by each finger is the half of the total pinch force, that is $4.70N/2 = 2.35N$. Thus, the difference with respect to the force measured using the same actuator (with a mean value of $2.69N$) and the one-finger platform is $0.34N$.

Analysis of results: Summarizing the obtained results, we can state that if we attempt to reproduce the pinch properties of the human hand, the actuator must fulfill the following features:

- The torque should be enough to produce a fingertip force of $2.96N$ with a time response of $0.244s$.
- The actuator should be suitable to produce a rotation of $\pi/2$ rad.

To calculate the required torque to apply a force of $2.96N$ using the proposed dynamic model, it is necessary to know the vector q, which corresponds to the dependent and independent coordinates of the robot and it is composed as shown in Eq. (6). Taking into account that the orientation of (x_i, y_i) is the same of (x_i', y_i'), we use the relations $x_i' = x_i + l_i \cos\theta_i/2$ and $y_i' = y_i + l_i \sin\theta_i/2$ to calculate the vector q. The values x_i, y_i and θ_i correspond to the measured kinematic information. As a result, applying the dynamic model, and using the kinematic DHKK-SRQ model, we found out that the torque $\tau_1(f_R, q, \dot{q}, \ddot{q}) = 74.5Nmm$.

5 Conclusions

We have presented the requirements for artificial muscles to design robotic fingers. This finger is under-actuated and based on human morphology according to artificial muscles. This finger is a mechanical chain with 3 joints driven with flexible wires to produce more adaptive grasping movements. The proposed kinematic and dynamic models allow us to calculate the torque requirement to mimic human finger force. Experiments compare pinch and achieved forces for 5 different servo motors. According to the obtained results and the performed analysis, we identify that smart materials (*e.g.* ionic polymer metal composite IPMC or shape memory alloy SMA) can fulfill the requirements of artificial muscles to design robotic hand prostheses. Consequently, we envisage the implementation of artificial muscles, based on smart materials, in the next prototype of our robotic finger.

Acknowledgements Through this acknowledgment, we express our sincere gratitude to the Université Paris Lumières UPL for the financial support through the project PROMAIN. This work has been partly supported by Université Paris Lumières UPL and by a Short Term Scientific Mission funding from LEME-UPO-EA4416 / LIASD-UP8-EA4383. We also acknowledge Colciencias - Colombia and the Universidad Militar Nueva Granada for the financial support of the PhD students.

References

1. T. Mouri, H. Kawasaki, and K. Umebayashi. Developments of new anthropomorphic robot hand and its master slave system. In *IEEE/RSJ International Conference on Intelligent Robots and Systems (IROS)*, pages 3225–3230, Alberta, Canada, Aug 2005. IEEE.
2. F. Röthling, R. Haschke, J.J. Steil, and H. Ritter. Platform portable anthropomorphic grasping with the bielefeld 20-dof shadow and 9-dof tum hand. In *IEEE/RSJ International Conference on Intelligent Robots and Systems (IROS)*, pages 2951–2956, San Diego, CA, USA, Nov 2007. IEEE.
3. T. Endo, H. Kawasaki, T. Mouri, Y. Ishigure, H. Shimomura, M. Matsumura, and K. Koketsu. Five-fingered haptic interface robot: Hiro iii. *IEEE Transactions on Haptics*, 4(1):14–27, 2011.
4. S.G. Nurzaman, F. Iida, C. Laschi, A. Ishiguro, and R. Wood. Soft robotics [tc spotlight]. *IEEE Robotics Automation Magazine*, 20(3):24–95, Sept 2013.
5. F. Ficuciello, G. Palli, C. Melchiorri, and B. Siciliano. Experimental evaluation of the UB Hand IV postural synergies. In *IEEE/RSJ International Conference on Intelligent Robots and Systems (IROS)*, pages 1775 – 1780, San Francisco, CA, USA, September 2011.
6. M.G. Catalano, G. Grioli, E. Farnioli, A. Serio, C. Piazza, and A. Bicchi. Adaptive synergies for the design and control of the Pisa/IIT SoftHand. *The International Journal of Robotics Research*, 33(5):768–782, 2014.
7. J. Reinecke, A. Dietrich, F. Schmidt, and M. Chalon. Experimental comparison of slip detection strategies by tactile sensing with the biotac® on the dlr hand arm system. In *IEEE International Conference on Robotics and Automation (ICRA)*, pages 2742–2748, Hong Kong, China, Jun 2014. IEEE.
8. C. Melchiorri, G. Palli, G. Berselli, and G. Vassura. Development of the UB Hand IV: Overview of Design Solutions and Enabling Technologies. *IEEE Robotics & Automation Magazine*, 20(3):72–81, September 2013.
9. J. Denavit and R. Hartenberg. A kinematic notation for lower-pair mechanisms based on matrices. *Trans. ASME Journal of Applied Mechanics*, 77:215–221, June 1955.
10. J. Ramirez, A. Rubiano, N. Jouandeau, M.N. El Korso, L. Gallimard, and O. Polit. Hybrid kinematic model applied to the under-actuated robotic hand prosthesis promain-i and experimental evaluation. In *14th IEEE/RAS-EMBS International Conference in reabilitation robotics (ICORR)*, Singapore, Aug 2015. IEEE.
11. V. Hugel and N. Jouandeau. Automatic generation of humanoids geometric model parameters. In *RoboCup 2013: Robot World Cup XVII*, pages 408–419. Springer, 2014.
12. J. Ramirez, A. Rubiano, N. Jouandeau, L. Gallimard, and O. Polit. Morphological optimization of prosthesis' finger for precision grasping of little objects. In *4th International workshop in medical and service robots (MESROB)*, Nantes, France, Jul 2015. Springer.
13. L. Yan and L. Xu. Study of diagonalization on skew self-conjugate matrix in quaternion field. In *Second International Conference on Computational Intelligence and Natural Computing Proceedings (CINC)*, volume 1, pages 72–75, Wuhan, China, 2010.
14. JO. Ramsay, X. Wang, and R. Flanagan. A functional data analysis of the pinch force of human fingers. *Applied Statistics*, 44:17–30, 1995.
15. T.A. Schreuders, M.E. Roebroeck, J. Goumans, J.F. van Nieuwenhuijzen, T. H. Stijnen, and H.J. Stam. Measurement error in grip and pinch force measurements in patients with hand injuries. *Physical therapy*, 83(9):806–815, 2003.